HHS Public Access

Author manuscript

Nature. Author manuscript; available in PMC 2016 May 06.

Published in final edited form as:

Nature. 2015 October 15; 526(7573): 439–442. doi:10.1038/nature15693.

Encoding of action by the Purkinje cells of the cerebellum

David J. Herzfeld[1], **Yoshiko Kojima**[2], **Robijanto Soetedjo**[2], and **Reza Shadmehr**[1]

[1] Department of Biomedical Engineering, Laboratory for Computational Motor Control, Johns Hopkins University School of Medicine, Baltimore, MD 21205, USA

[2] Department of Physiology and Biophysics, Washington National Primate Center, University of Washington, Seattle, WA 98195, USA

Summary

Execution of accurate eye movements depends critically on the cerebellum[1,2,3], suggesting that Purkinje cells (P-cells) may predict motion of the eye. Yet, this encoding has remained a long-standing puzzle: P-cells show little consistent modulation with respect to saccade amplitude[4,5] or direction[4], and critically, their discharge lasts longer than duration of a saccade[6,7]. Here, we analyzed P-cell discharge in the oculomotor vermis of behaving monkeys[8,9] and found neurons that increased or decreased their activity during saccades. We estimated the combined effect of these two populations via their projections on the caudal fastigial nucleus (cFN) and uncovered a simple-spike population response that precisely predicted the real-time motion of the eye. When we organized the P-cells according to each cell's complex-spike directional tuning, the simple-spike population response predicted both the real-time speed and direction of saccade multiplicatively via a gain-field. This suggests that the cerebellum predicts the real-time motion of the eye during saccades via the combined inputs of P-cells onto individual nucleus neurons. A gain-field encoding of simple spikes emerges if the P-cells that project onto a nucleus neuron are not selected at random, but share a common complex-spike property.

Keywords

simple-spikes; Purkinje cells; oculomotor vermis; saccade; cerebellum

Previous studies have focused on bursting activity of Purkinje-cells (P-cells) during saccadess[6,10,11] and found no consistent modulation with saccade amplitude[4,5], speed[5–7], or direction[4]. A recent simulation[12] suggested that P-cells that pause during saccades may be important in understanding the responses observed in the deep cerebellar nucleus neurons.

Correspondence: David Herzfeld, 416 Traylor Building, Johns Hopkins School of Medicine, 720 Rutland Ave., Baltimore, MD 21205, USA. dherzfe1@jhmi.edu; Phone: 410-614-3424; Fax: 410-502-2826. Correspondence and requests for materials should be addressed to R. Shadmehr (shadmehr@jhu.edu)..

Author contributions: Y. Kojima and R. Soetedjo conceived, designed, and performed all experiments. D. Herzfeld and R. Shadmehr formed the conceptual model. D. Herzfeld analyzed the data and made all figures. R. Shadmehr and D. Herzfeld wrote the paper.

Author information: The authors have declared no conflicts of interest.

The main puzzle that we wished to tackle was how the P-cells encoded the real-time motion of the eye.

We analyzed simple-spike activity of 72 oculomotor vermis (OMV, cerebellar lobules VI and VII) P-cells from five monkeys during saccades. Our population included cells that exhibited increased activity (bursting; n=39, Fig. 1a) or decreased activity (pausing; n=33, Fig. 1b). Consistent with previous reports[5,6,10], the majority of the neurons were poorly modulated by saccade amplitude (Fig. 1c, and Extended Data Fig. 1). However, the mean firing rate of burst cells (but not pause cells) increased significantly with saccade peak speed (Fig. 1d, $p<10^{-10}$). Previous work had demonstrated that the population response encoded additional saccade-related information that was not reliably present in the responses of individual neurons[6,13,14]. To examine the population response, we measured change in firing rates (from baseline) for the bursting and pausing cells during slow (400°/s) and fast (650°/s) saccades (Fig. 1e), pooled across all directions. The onset of change in firing rates in both populations generally led saccade onset by more than 50ms. The termination of activity was also significantly later than the saccade: a 650°/s saccade was 38±1.2ms in duration (mean ±SEM), whereas activity of burst and pause cells persisted for a more than 100ms. Given that the cerebellum is thought to play a critical role in termination of ipsiversive saccades[15,16], how can P-cells be involved in controlling the eye if their activity persists so much longer than the saccade?

P-cells project to the caudal fastigial nucleus (cFN), where about 50 P-cells converge onto a cFN neuron[17]. For each P-cell we computed the probability of a simple-spike in 1ms time-bins during saccades of a given peak speed, averaged across all directions. We then chose 50 P-cells at random and computed the total number of simple-spikes generated by the population at each millisecond of time, resulting in an estimate of the rate of presynaptic spikes converging onto a cFN cell. The results (Fig. 1f) revealed a real-time encoding of the speed of the eye: the peak of the activity preceded peak speed, increased in magnitude when speed increased, and returned to baseline just before saccade termination (R^2 at the optimal delay, 400 deg/s: $R^2=0.52$, $p<10^{-22}$; 650 deg/s: $R^2=0.62$, $p<10^{-43}$). It appeared that the simple-spikes of the pause and burst cells combined together to predict motion of the eye.

Let us hypothesize that the P-cells that project to a nucleus neuron are not selected randomly, but are organized by their inputs from the inferior olive[18]. That is, suppose that the olive projections divide the P-cells into clusters where each cluster of P-cells projects onto a single nucleus neuron. The input from the olive produces complex-spikes (CS) in the P-cells. We found that if we organized the simple-spikes of the P-cells based on each cell's CS properties, additional features of the population activity were unmasked.

We measured CS properties of each P-cell by inducing a post-saccadic error through displacement of the target during the saccade, and then measured the probability of CS as a function of the direction of this error (Fig. 2) (Supplementary information section 2). For each P-cell, the direction of error that produced the largest probability of a CS during the 50-200ms post-saccade period was labeled as CS-on, and the opposite direction was labeled as CS-off[9] (Extended Data Fig. 2). We then made the assumption that the P-cells that projected onto a nucleus neuron all had the same CS-on direction (Fig. 3a). Under this

assumption, we computed the rate of presynaptic simple-spikes that a nucleus neuron would receive from the cluster of P-cells (Supplementary Information section 3). We did this by convolving each P-cell simple-spike train with a 2.5ms standard-deviation normalized Gaussian, approximating the temporal characteristics of the inhibition produced in the nucleus neuron due to a simple-spike in the P-cell[17,19].

Fig. 3b shows the change in population response from baseline when a saccade was made in the same direction as CS-off. The response rose above baseline before saccade onset, peaked prior to peak speed, and then returned to near baseline. The peak response scaled robustly with saccade amplitude (Fig. 3c, R^2=0.93, $p<10^{-5}$). We observed a strong correspondence between the real-time population response and the real-time speed (lower plot of Fig. 3d, Extended Data Fig. 3). The population response led eye speed by an average of 21.2±0.4ms (correlation analysis in the CS-off direction, mean±SEM). Peak population response precisely predicted peak speed (Fig. 3e, R^2=0.98, $p<10^{-7}$).

We took advantage of natural variability in saccades to further test the relationship between the population response and speed. We sorted all 10° saccades (direction CS-off) according to peak speed (Fig. 3f) and found that despite the constant amplitude, the population response precisely predict the actual peak speed of the eye (Fig. 3g, R^2=0.96, $p<10^{-7}$). Therefore, when the simple-spikes were organized according to each cell's CS directional preference, the population response for saccades of constant direction predicted nearly all of the variability in saccade peak speed.

No previous work, to our knowledge, had revealed how direction of a saccade is encoded in the activity of P-cells. For the burst and pause cells, the mean and peak firing rates during the saccade did not vary as a function of direction (Extended Data, Fig. 4). However, organizing the population response according to each P-cell's CS tuning preference revealed a clear encoding of direction: the peak response was greater if the saccades were in the same direction as CS-off as compared to CS-on (Fig. 4a, t-test $p<10^{-16}$). Indeed, the peak population response rose linearly as a function of peak speed in both directions, but with a larger gain when the saccade direction was congruent with CS-off (Fig. 4b, RM-ANOVA with main effects of peak-speed, $p<10^{-15}$; CS-direction $p<10^{-7}$; and a speed by CS-direction interaction, $p<10^{-15}$).

To more closely examine the effects of saccade direction, we plotted the population response across saccade directions with respect to CS-on (Fig. 4c). We found that the population response was highest for saccades made in the CS-off direction, with an encoding of direction that resembled a cosine function (Fig. 4d). Therefore, the combined activity of burst and pause cells, but not the activity of either population individually (Extended Data Fig. 4), aligned to CS-off, produced a population response that exhibited gain-field encoding: the magnitude of the population response increased linearly with speed, and was cosine tuned in direction, with a multiplicative interaction between speed and direction. The rate of simple-spikes converging onto cFN, represented by $s(t)$, predicted in real-time motion of the eye (Supplementary Information, Section 4, Extended Data Fig. 5):

$$\begin{aligned} s\left(t\right) &= \left|\dot{\mathbf{x}}\left(\mathbf{t}+\boldsymbol{\Delta}\right)\right| g\left(\theta,\theta_{cs}\right)+c \\ g\left(\theta,\theta_{cs}\right) &= a\,cos\left(\theta,\theta_{cs}\right)+b \end{aligned} \quad (1)$$

In this equation, $|\dot{\mathbf{x}}(t+\Delta)|$ represents the magnitude of the eye velocity vector at time $t+\Delta$ (where $\Delta = 19$ ms), b and c are baseline offsets, a is a scaling factor, θ is saccade direction, and θ_{CS} is direction of CS-off for that cluster of P-cells. The resulting gain-field encoding of eye motion is depicted in Fig. 4e.

How did the activity of individual cells produce this directional encoding in the population response? The main contributors were the pause cells, which started their pause approximately 10ms earlier when the saccade was in the CS-on direction (Fig. 4f), a change which was independent of saccade speed (Extended Data Fig. 6). This subtle shift in the timing of spikes produced an increase of the population response when saccade direction changed from CS-on to CS-off (Fig. 4a).

We found that the anatomical distribution of P-cells, as labeled by their CS-off direction, was not random, but lateralized[9] (Extended Data Fig. 7), confirming previous anatomical studies suggesting that olivary projections are contralateral[20,21]. P-cells with rightward CS-off were more likely to be on the right side of the cerebellum (t-test, $p<10^{-4}$). This indicates that saccades made in the same direction as CS-off were typically ipsiversive whereas saccades congruent with CS-on were contraversive. In contrast, pause and burst cells were uniformly distributed across the cerebellum ($p>0.4$).

Our results rely critically on our hypothesis that P-cells organize into clusters with roughly equal number of pause and burse cells, all with a common complex-spike tuning preference (Fig. 3a). If, contrary to our hypothesis, pause and burst cells organized into separate clusters, the population response would not predict the real-time motion of the eye (Fig. 1e). Similarly, if each cluster was not composed of roughly equal number of pause and burst cells, the population response could not predict the real-time speed of the eye (Extended Data Fig. 8, Supplementary Information section 5). The fact that burst and pause cells were distributed uniformly across the recording locations, and not lateralized as we found with the CS tuning properties, suggests that a cluster is composed of both burst and pause. Finally, if we ignored the CS properties of the P-cells, and made the typical assumption that simple-spikes were sufficient to uncover the coordinate system of encoding motion, then the gain-field representation of speed and direction would disappear (Extended Data Fig. 9, Supplementary information section 6).

In summary, organizing the P-cell into clusters where all the cells shared a common complex-spike property resulted in simple spikes that encoded speed and direction in real-time via a gain-field.

Together, our results suggest three principles of cerebellar function during control of saccadic eye movements. First, the cerebellum predicts real-time motion not in the time-course of individual P-cell simple-spikes, nor in the individual activities of the bursting or pausing populations, but in the combined activities of these two populations via the simple-spikes that converge onto cells in the deep cerebellar nucleus. A similar population coding

has been suggested during smooth pursuit[22]. Second, this population input to each nucleus neuron encodes direction and speed via a gain-field. Because a similar encoding has been shown in the posterior parietal cortex during saccades[23], as well as in the motor cortex during reaching[24], our observation in the cerebellum suggests a common principle of encoding in disparate regions of the motor system. Finally, the gain-field encoding was present if we assumed a specific anatomical organization: a cluster of P-cells that projected onto a single nucleus neuron was composed of approximately equal numbers of bursting and pausing P-cells, all sharing a common complex-spike property. Because the complex-spikes of a P-cell are due to input from the inferior olive, the gain-field encoding predicts that the oculomotor vermis is organized into clusters of P-cells that share similar climbing fiber projections from the inferior olive. This in turn suggests that motor memories are anatomically clustered in the cerebellum by the errors that were experienced during movements[25].

Methods

We analyzed extra-cellular recordings from P-cells of the oculomotor vermis in five rhesus monkeys (B, F, W, K, KO) while they made saccades to visual targets[8,9] (Supplementary Information, Section 1). Each cell was well isolated for an average of 3000 saccades. Briefly, a scleral search coil was surgically attached to the eye of each monkey, allowing measurement of eye position[26] while the animal's head was restrained. Following surgery, the monkeys were trained to make saccades to targets of varying amplitudes and directions. We identified P-cell activity in OMV by their saccade related change in the simple-spike response, as well as the presence of complex-spikes. Neurophysiological data were sampled at 50 kHz. All experiments were performed in accordance with the Guide for the Care and Use of Laboratory Animals (1997) and exceeded the minimal requirements recommended by the Institute of Laboratory Animal Resources and the Association for Assessment and Accreditation of Laboratory Animal Care International. All animal procedures were approved by the local committee at the University of Washington.

The CS-on direction for each cell was determined using the standard intra-saccadic step paradigm[27], in which the target was displaced during the initial saccade (Fig. 2). This error resulted in complex-spikes during the period following the saccade, when the monkey observed the error. For every cell, we determined the CS-on direction as the error direction which elicited the largest probability of CS during the 50-200ms following the primary saccade. For n=39 cells we were able to maintain excellent isolation of the P-cell throughout the experiment, allowing us to perform automated identification of CSs on every trial. This allowed us to compute the probability of complex-spikes as a function of error direction. For the remaining n=33 cells, the CS-on direction was determined via analysis of the initial 50 trials for each direction of error[8]. CS-off was defined as CS-on+180°.

We computed firing rates by determining the inverse of the time between two consecutive simple-spikes[28] and then convolved the resulting time series with a normalized Gaussian kernel with a standard deviation of 2.5ms, which is significantly shorter than conventional kernels[6]. This guarded against over-estimating the duration of a population response. We calculated the mean firing rate during the saccade by taking the average of the firing rate

from the start to the end of the saccade. We determined the peak response of a P-cell as the maximum firing during the saccade period.

The response of an individual P-cell is quite variable[8], with some neurons showing a combination of bursting and pausing activity in the time period near saccade onset. Therefore, in order to categorize neurons exclusively as pausing or bursting, we compared the mean firing rate of each cell from the period [200–100]ms prior to saccade onset of all recorded trials to a 150ms period centered on saccade peak speed. Neurons that reduced their rate during this extended period were classified as ‘pausing’ whereas neurons that significantly exceeded this rate were classified as ‘bursting’. We tested this categorization statistically via a paired t-test with a cutoff of $p=0.05$. Only two neurons (both bursting) did not pass this statistical test. We included these two neurons in the bursting population.

To establish confidence intervals on the population responses, we performed a bootstrap analysis in which we randomly sampled 50 neurons from the available pool of 72 (with replacement), which simulated the approximate number of P-cell inputs that project onto a nucleus neuron[17]. Error bars show mean±SEM of 50 bootstrapped P-cell populations. In cases where we show the responses of the bursting/pausing populations separately, we report the mean±SEM across neurons in the respective population without bootstrapping.

To compute the population response of a cluster of 50 P-cells, we first convolved the simple-spikes of each P-cell with a kernel (normalized Gaussian of 2.5ms standard deviation), approximately representing the time-course of post-synaptic inhibition induced by the simple-spike train[17]. We then computed the change from baseline for each cell, and finally the sum of changes across the population, resulting in a population response that had units of spikes/sec, computed at each millisecond of time.

Extended Data

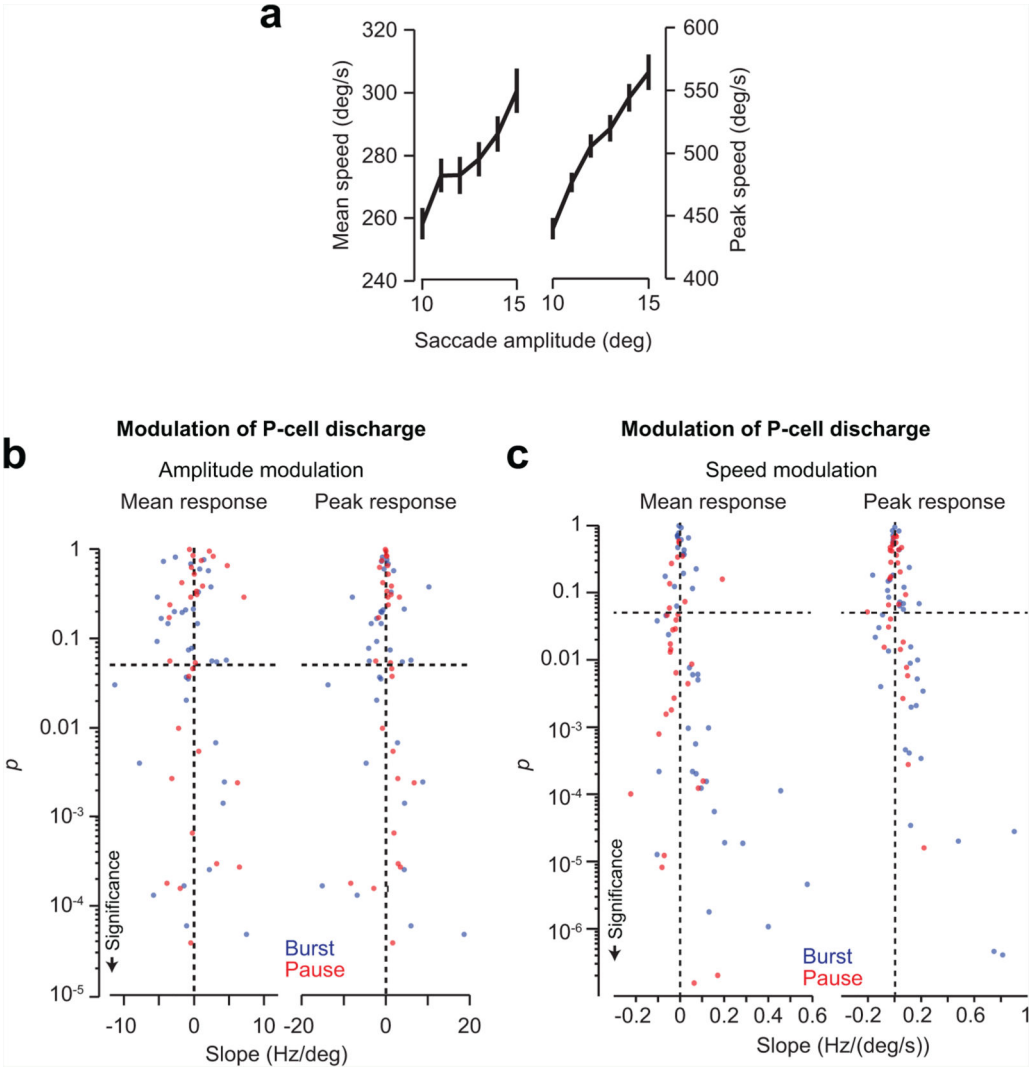

Extended Data Figure 1.

Firing rates of individual P-cells as a function of saccade amplitude and peak speed. **a**. Increase in saccade amplitude produced robust increases in mean and peak saccade speed (mean: $R^2 = 0.86$, $p < 10^{-4}$; peak: $R_2 = 0.99$, $p < 10^{-9}$). **b**. For each neuron, we correlated the average firing rate and the peak firing rate (computed over the saccade duration and averaged over all directions) with saccade amplitude. Some neurons increased their firing rates with increasing saccade amplitude (positive slope) and some neurons decreased their responses (negative slope). However, mean and peak firing rates of a majority of neurons (47/72) were not significantly modulated with saccade amplitude. As a result, activity of neither the burst nor the pause cells showed a significant modulation with saccade amplitude (Fig. 1c, main manuscript). **c**. Majority of neurons (45/72) had a significant linear relationship between firing rates and peak saccade speed. In particular, mean and peak response of burst cells showed a significant increase with peak speed (Fig. 1d, main manuscript).

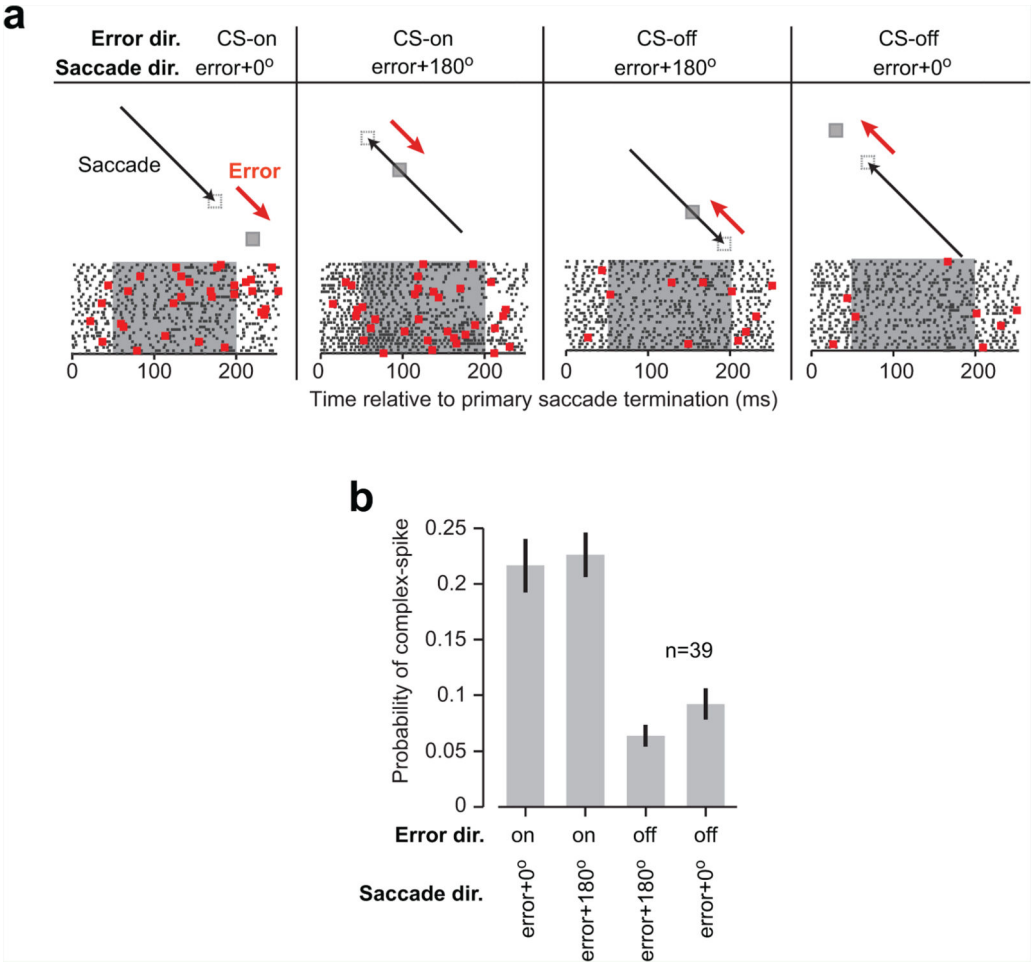

Extended Data Figure 2.

Complex spikes encode direction of error, not direction of saccade that preceded that error. **a**. The response of the same cell shown in Fig. 2 as a function of direction of saccade and direction of error. The probability of CS is high when the direction of error is at −45°, despite the fact that saccade direction may be at −45° or +135°. **b.** Population statistics from n=39 P-cells in which the probability of CS was quantified as a function of direction of the error vector and direction of the saccade that preceded that error. Probability of CS depended on direction of error, not direction of saccade.

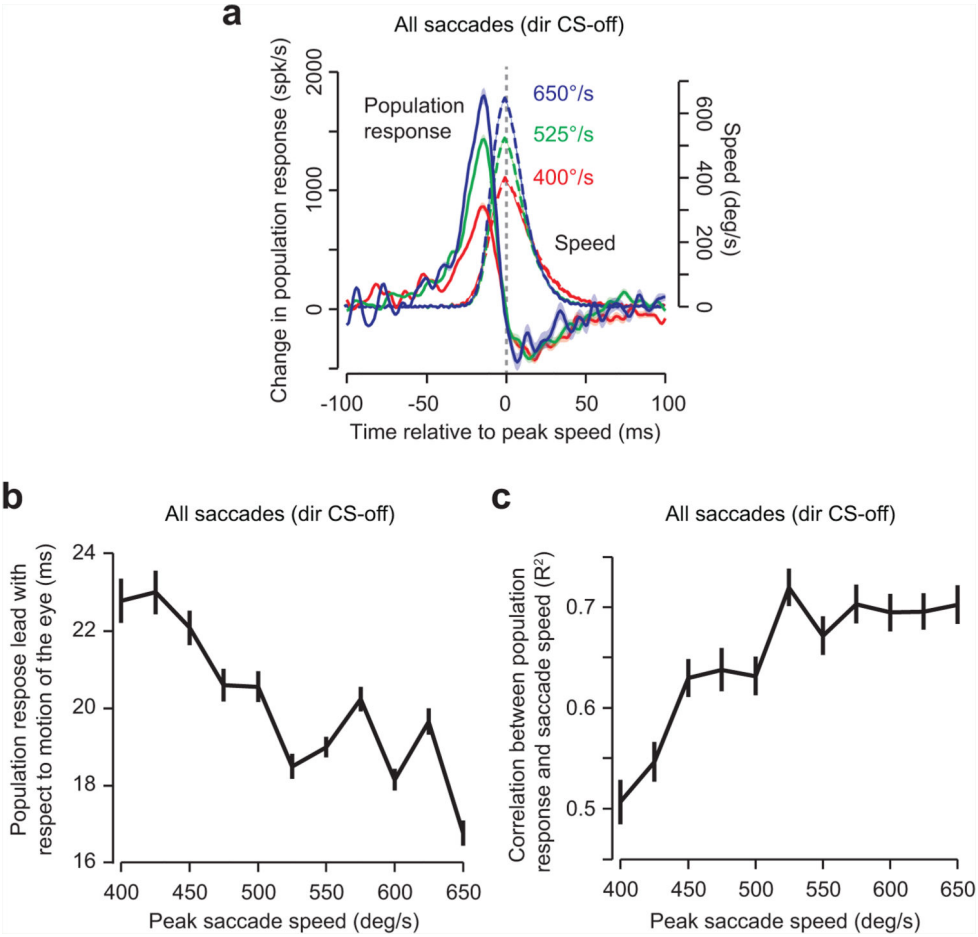

Extended Data Figure 3.

The simple-spike population response of P-cells, organized by their complex-spike properties (Fig. 3a), correlated with motion of the eye in real-time. **a**. Population response for saccades in direction CS-off for three different peak speeds. **b**. Temporal lead of the population response with respect to saccade speed as computed by finding the temporal shift that maximized the cross-correlation. **c.** Correlation between the population response and the temporally shifted eye speed trace (measured as R^2).

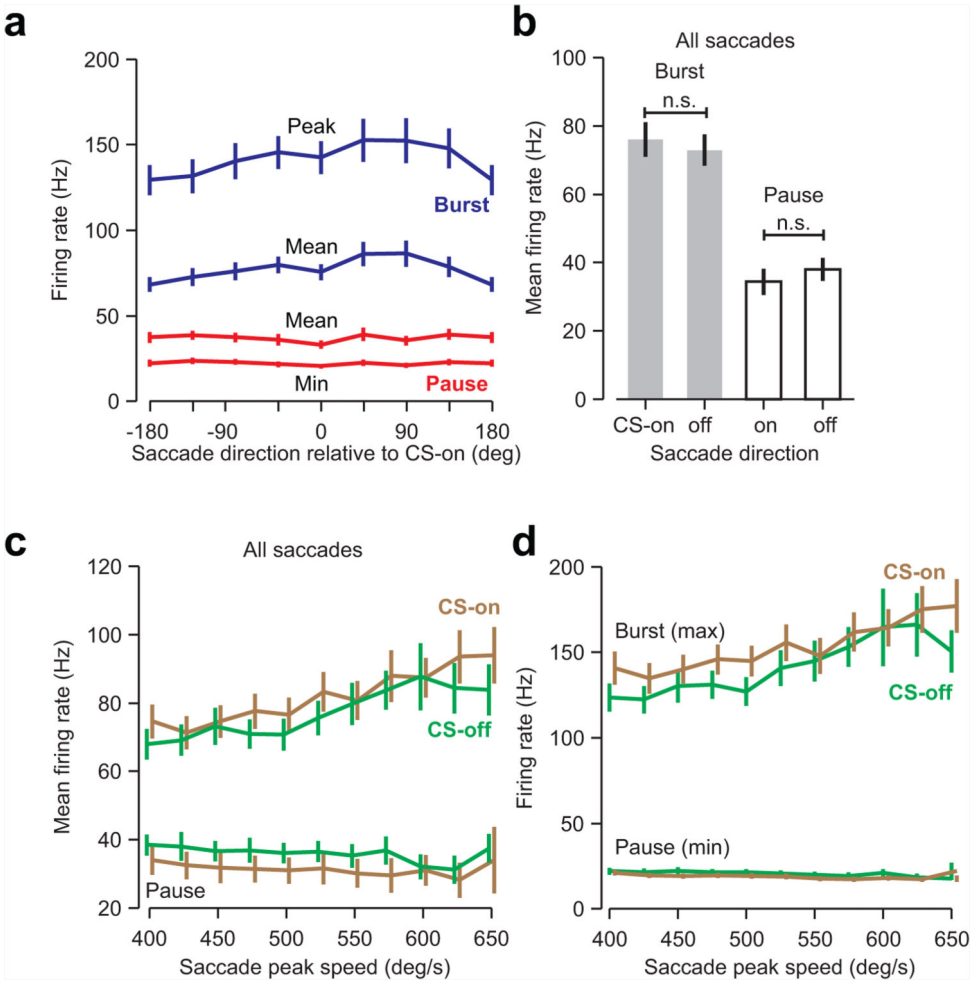

Extended Data Figure 4.

Mean and peak/trough firing rate of the burst and pause cells were poorly modulated by saccade direction. **a**. Maximum, minimum, and mean firing rates averaged across burst or pause cells with respect to saccade direction, relative to CS-on direction of each cell. **b.** Mean firing rates of the burst and pause cells, as measured across all saccades, were not significantly different for saccades in the CS-on vs. CS-off direction (burst $p > 0.10$, pause $p > 0.05$). **c**. Mean firing rates of the burst and pause cells as a function of saccade speed, for saccades in the CS-on vs. CS-off direction. Saccade speed modulated mean firing rates of the burst cells, but there were no significant interaction between saccade direction and speed ($p > 0.6$), nor a significant effect of saccade direction ($p > 0.7$). **d.** Peak (maximum) firing rates of the burst cells and the minimum firing rate of the pause cells as a function of saccade speed, for saccades in the CS-off and CS-on directions. We asked whether the maximum response of the burst cells or the minimum response of the pause cells was significantly modulated by direction. Separate RM-ANOVAs showed that for the burst cells, peak activity increased as a function of saccade peak speed ($p < 0.001$), but this relationship was unaffected by saccade direction ($p > 0.4$). For the pause cells, the response was not affected by saccade speed ($p > 0.6$), and this relationship was not modulated by saccade

direction ($p > 0.4$). In summary, we found that saccade direction did not significantly alter the encoding of peak speed in either the mean or minimum/maximum activity of P-cells.

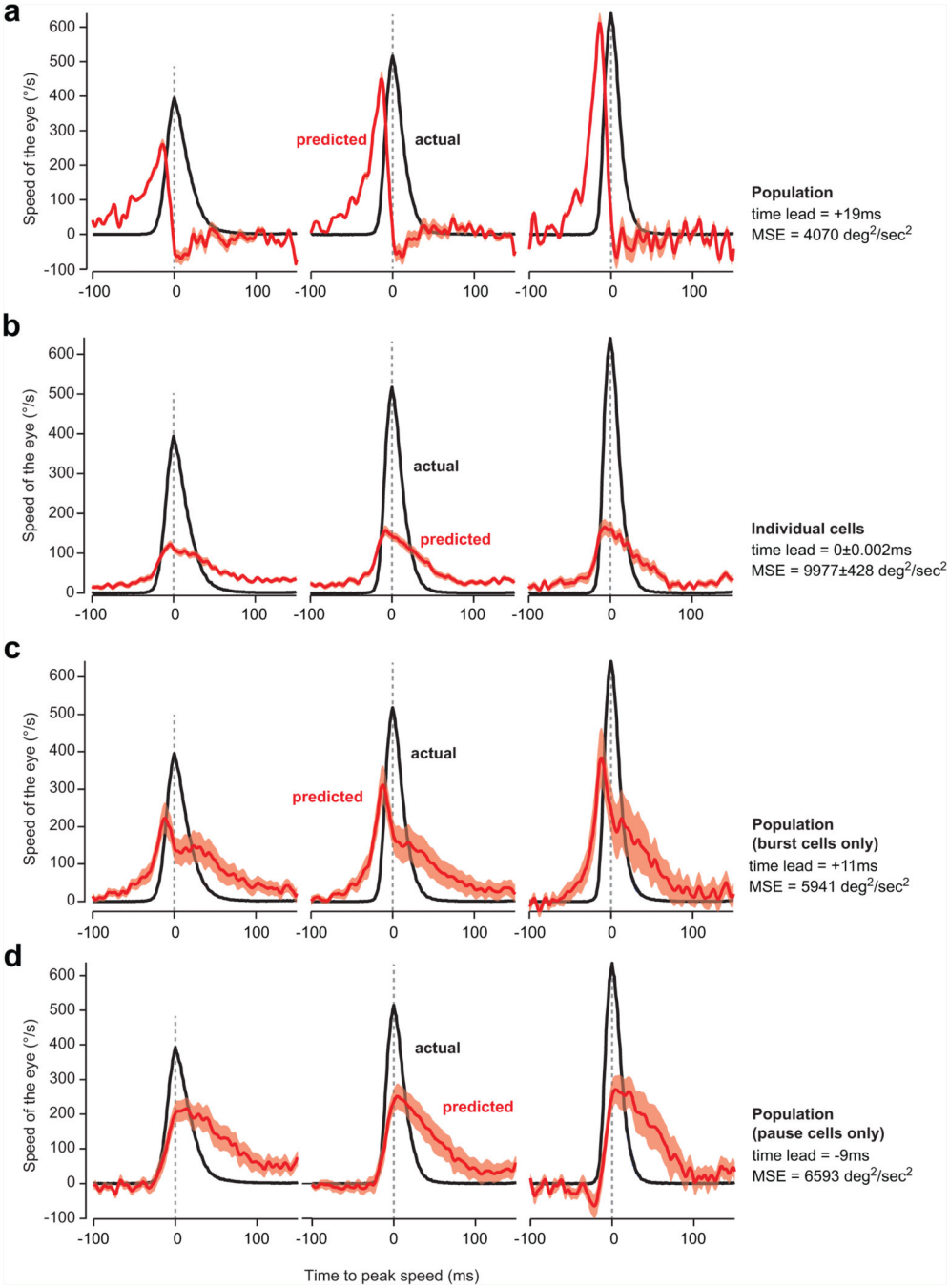

Extended Data Figure 5.

Population of P-cells, organized by their complex spike properties, predicted the real-time speed of the eye better than activity of individual cells. **a.** We employed Eq. (S2) and used the measured population response $s(t)$ of P-cells to predict the real-time speed of the eye $|\hat{\dot{\mathbf{x}}}(\mathbf{t}+\boldsymbol{\Delta})|$. The plot shows the predicted speed for saccades of 400, 525, and 650 deg/sec.

The predicted speed led the actual speed by 19ms. MSE is the mean squared error between the predicted and actual eye trajectory at the optimal value of Δ. **b.** The result of fitting Eq. (S2) to the response of individual neurons. **c.** The result of fitting Eq. (S2) to the discharge of a population composed exclusively of burst cells. **d.** The result of fitting Eq. (S2) to the discharge of a population composed exclusively of pause cells.

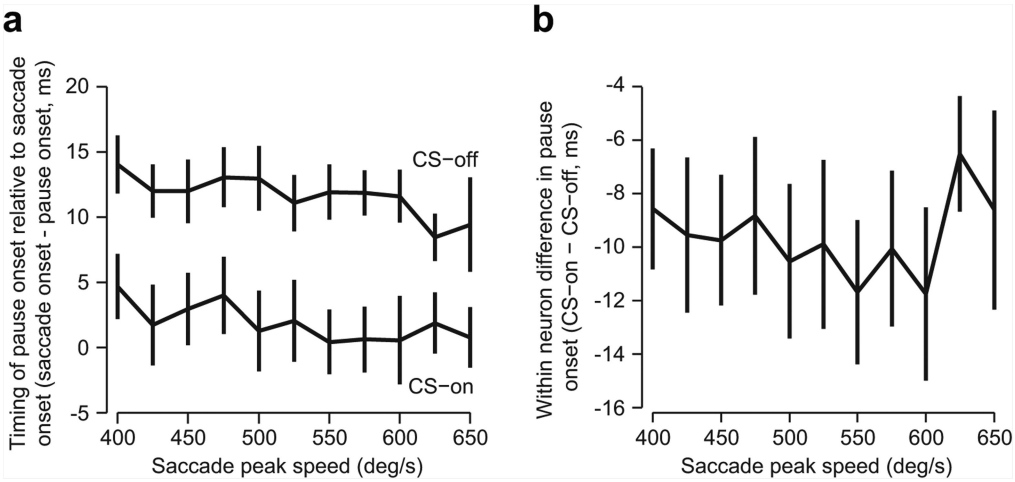

Extended Data Figure 6.

Change in saccade direction was associated with a change in the timing of the reduction of discharge in the pause cells, i.e., pause onset (see Fig. 4f). **a.** Timing of pause onset with respect to saccade onset for saccades of various speeds and directions. We computed the pause onset as the time when the neuron's response reached 20% of its minimum response. Positive numbers indicate that the pause onset occurred before saccade onset. **b.** Within neuron measure of pause onset for saccade in direction CS-on, minus onset from saccades in direction CS-off. Negative numbers indicate that the pause onset occurred earlier for saccades in the CS-on direction.

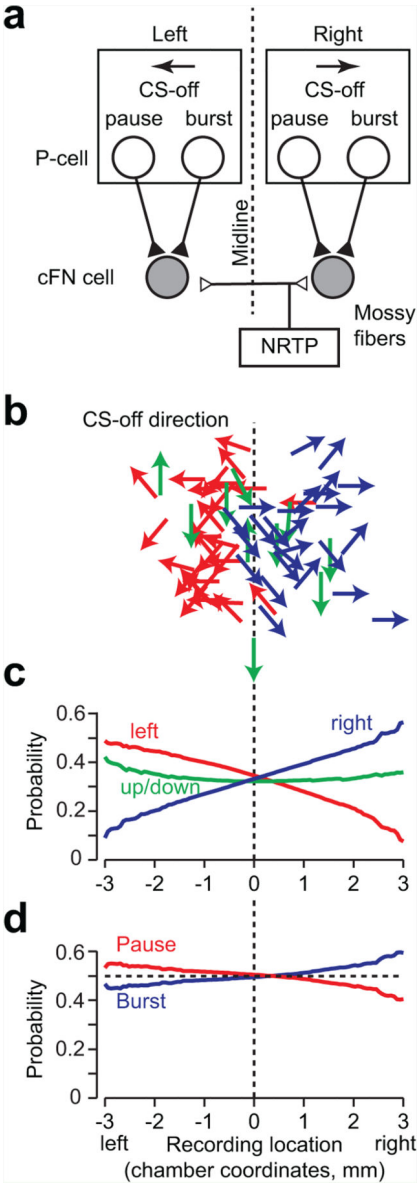

Extended Data Figure 7.

CS-dependent organization of the P-cells. **a.** Hypothesized anatomical organization of the oculomotor vermis (OMV). Bursting and pausing P-cells are organized into clusters, with the cells in each cluster sharing a common CS direction. Neurons on the right side of the OMV project to right cFN neurons and have CS-off directions to the right. **b.** Distribution of the CS-off directions from recorded neurons in chamber coordinates. Vertical dotted line shows the line which best separates rightwards CS-off direction neurons (blue) from leftwards CS-off direction neurons (red). **c.** Probability of having a rightwards (blue), up/down (green) or leftwards CS-off direction as a function of chamber coordinates. P-cells with CS-off to the left were more probable on the left side of the cerebellum. P-cells with CS-off to the right were more probable on the right-side of the cerebellum. **d.** Pause (red) and burst (blue) P-cells were equally likely at all recorded locations.

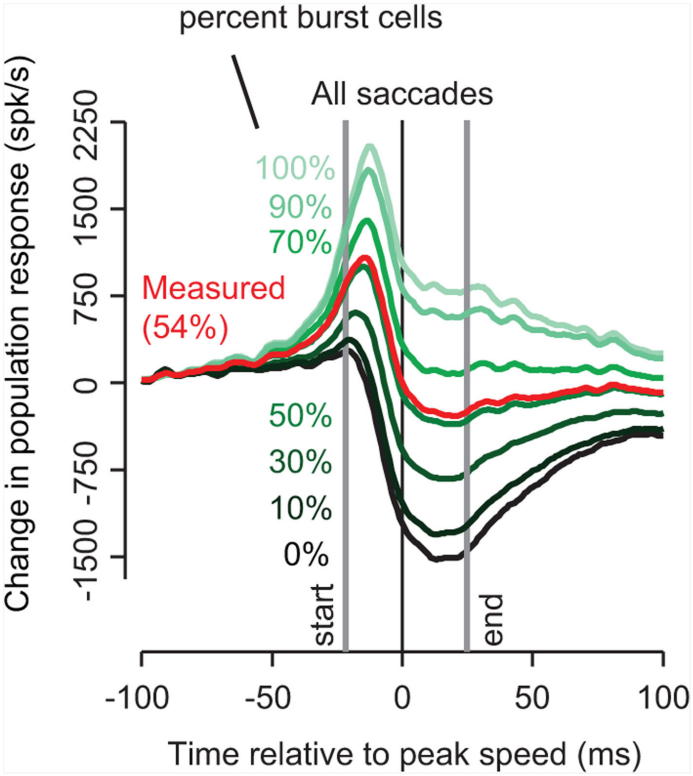

Extended Data Figure 8.

The population response was sensitive to the fraction of pause and burst cells that composed a cluster of P-cells. In our data set, 54% of the population was composed of burst cells. We computed the population response under the assumption that the membership of a cluster was 54% burst cells. Here, we tested how sensitive the population response was to this membership ratio. The vertical lines indicate saccade onset and offset for all saccades pooled across direction and speed. As the percentage of burst cells in the cluster becomes larger than 70%, or smaller than 50%, the population response no longer returns to baseline at saccade offset.

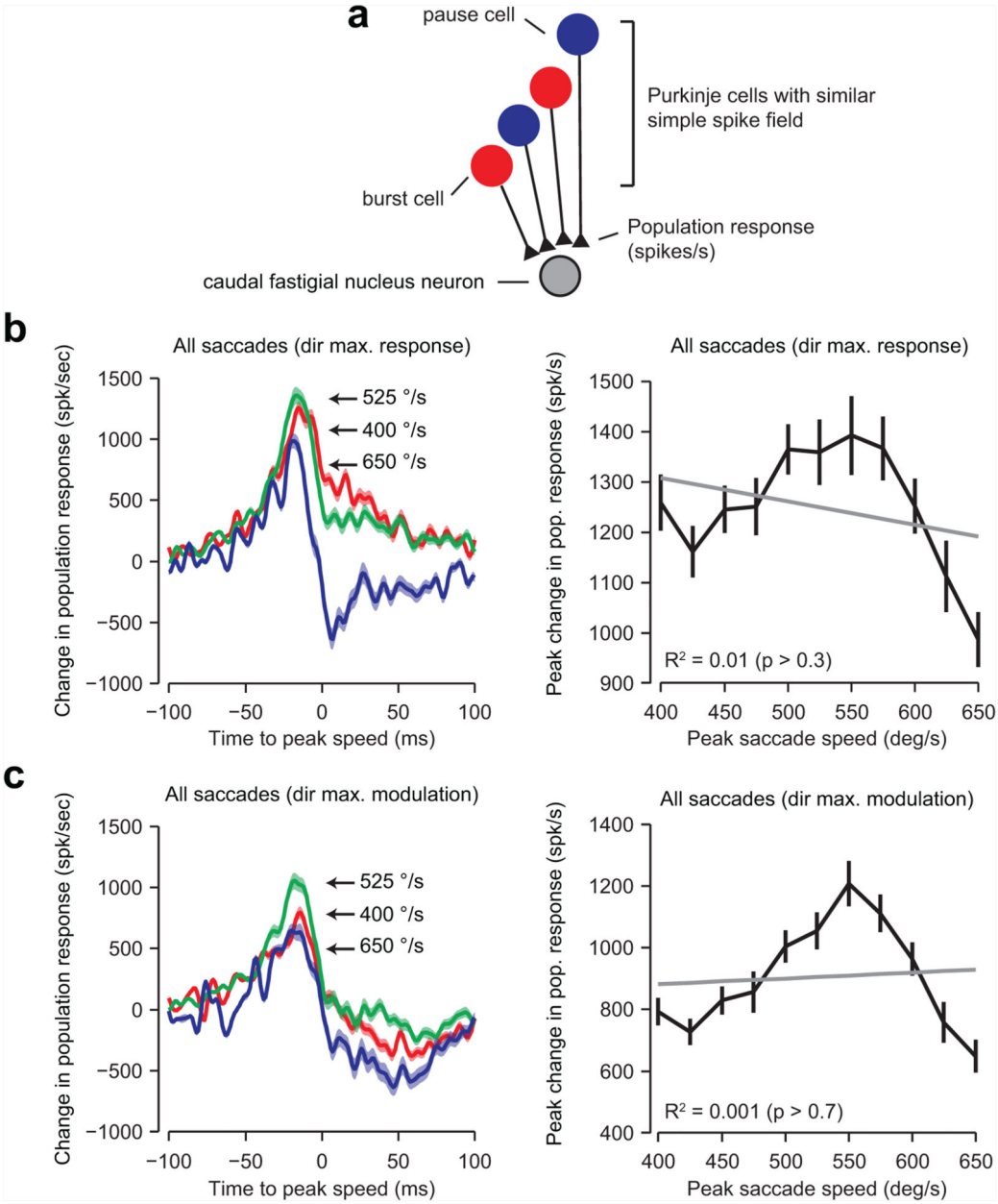

Extended Data Figure 9.

Gain-field encoding of saccade kinematics in the population response of the P-cells disappeared if the P-cells were organized by their simple-spike activity. **a.** In this analysis we assumed that a collection of 50 P-cells projected onto a single cFN neuron, with the property that all the P-cells shared a similar simple-spike preferred direction. Therefore, the cluster was organized based on the simple-spike properties of the P-cells, not their complex-spike properties. **b**. The population response for saccades made in the direction for which each P-cell showed the largest mean firing rate (simple-spikes), for various saccade peak speeds. The peak population response was not modulated with saccade speed. Error bars are boot-strap estimated SEM. **c.** The population response for saccades made in the direction of maximal modulation. For burst cells, this was the direction for which the P-cell showed the

largest mean firing rate, whereas for pause cells, this was the direction associated with the minimum activity (largest pause). The peak population response was not modulated with saccade speed when clusters were organized based on the direction of maximal simple-spike modulation.

Supplementary Material

Refer to Web version on PubMed Central for supplementary material.

Acknowledgements

These data were collected in the laboratory of Albert Fuchs. The authors are very grateful to his generosity. The authors would like to thank Sascha du Lac for her comments. The work was supported by NIH grants R01NS078311, R01EY019258, R01EY023277, and F31NS090860.

References

1. Xu-Wilson M, Chen-Harris H, Zee DS, Shadmehr R. Cerebellar Contributions to Adaptive Control of Saccades in Humans. J. Neurosci. 2009; 29:12930–12939. [PubMed: 19828807]
2. Barash S, et al. Saccadic Dysmetria and Adaptation after Lesions of the Cerebellar Cortex. J. Neurosci. 1999; 19:10931–10939. [PubMed: 10594074]
3. Kojima Y, Soetedjo R, Fuchs AF. Effects of GABA agonist and antagonist injections into the oculomotor vermis on horizontal saccades. Brain Res. 2010; 1366:93–100. [PubMed: 20951682]
4. Ohtsuka K, Noda H. Discharge properties of Purkinje cells in the oculomotor vermis during visually guided saccades in the macaque monkey. J. Neurophysiol. 1995; 74:1828–1840. [PubMed: 8592177]
5. Helmchen C, Büttner U. Saccade-related Purkinje cell activity in the oculomotor vermis during spontaneous eye movements in light and darkness. Exp. Brain Res. 1995; 103:198–208. [PubMed: 7789427]
6. Thier P, Dicke PW, Haas R, Barash S. Encoding of movement time by populations of cerebellar Purkinje cells. Nature. 2000; 405:72–76. [PubMed: 10811220]
7. Kase M, Miller DC, Noda H. Discharges of Purkinje cells and mossy fibres in the cerebellar vermis of the monkey during saccadic eye movements and fixation. J. Physiol. 1980; 300:539–555. [PubMed: 6770085]
8. Kojima Y, Soetedjo R, Fuchs AF. Changes in Simple Spike Activity of Some Purkinje Cells in the Oculomotor Vermis during Saccade Adaptation Are Appropriate to Participate in Motor Learning. J. Neurosci. 2010; 30:3715–3727. [PubMed: 20220005]
9. Soetedjo R, Kojima Y, Fuchs AF. Complex Spike Activity in the Oculomotor Vermis of the Cerebellum: A Vectorial Error Signal for Saccade Motor Learning? J. Neurophysiol. 2008; 100:1949–1966. [PubMed: 18650308]
10. Catz N, Dicke PW, Thier P. Cerebellar-dependent motor learning is based on pruning a Purkinje cell population response. Proc. Natl. Acad. Sci. 2008; 105:7309–7314. [PubMed: 18477700]
11. Catz N, Dicke PW, Thier P. Cerebellar Complex Spike Firing Is Suitable to Induce as Well as to Stabilize Motor Learning. Curr. Biol. 2005; 15:2179–2189. [PubMed: 16360681]
12. Gad YP, Anastasio TJ. Simulating the shaping of the fastigial deep nuclear saccade command by cerebellar Purkinje cells. Neural Netw. 2010; 23:789–804. [PubMed: 20542662]
13. Dash S, Dicke PW, Thier P. A vermal Purkinje cell simple spike population response encodes the changes in eye movement kinematics due to smooth pursuit adaptation. Front. Syst. Neurosci. 2013; 7:3. [PubMed: 23494070]
14. Prsa M, Dash S, Catz N, Dicke PW, Thier P. Characteristics of Responses of Golgi Cells and Mossy Fibers to Eye Saccades and Saccadic Adaptation Recorded from the Posterior Vermis of the Cerebellum. J. Neurosci. 2009; 29:250–262. [PubMed: 19129401]

15. Robinson FR, Straube A, Fuchs AF. Role of the caudal fastigial nucleus in saccade generation. II. Effects of muscimol inactivation. J. Neurophysiol. 1993; 70:1741–1758. [PubMed: 8294950]
16. Fuchs AF, Robinson FR, Straube A. Role of the caudal fastigial nucleus in saccade generation. I. Neuronal discharge pattern. J. Neurophysiol. 1993; 70:1723–1740. [PubMed: 8294949]
17. Person AL, Raman IM. Purkinje neuron synchrony elicits time-locked spiking in the cerebellar nuclei. Nature. 2012; 481:502–505. [PubMed: 22198670]
18. De Zeeuw CI, et al. Spatiotemporal firing patterns in the cerebellum. Nat. Rev. Neurosci. 2011; 12:327–344. [PubMed: 21544091]
19. Telgkamp P, Padgett DE, Ledoux VA, Woolley CS, Raman IM. Maintenance of High- Frequency Transmission at Purkinje to Cerebellar Nuclear Synapses by Spillover from Boutons with Multiple Release Sites. Neuron. 2004; 41:113–126. [PubMed: 14715139]
20. Yamada J, Noda H. Afferent and efferent connections of the oculomotor cerebellar vermis in the macaque monkey. J. Comp. Neurol. 1987; 265:224–241. [PubMed: 3320110]
21. Kralj-Hans I, Baizer JS, Swales C, Glickstein M. Independent roles for the dorsal paraflocculus and vermal lobule VII of the cerebellum in visuomotor coordination. Exp. Brain Res. 2006; 177:209–222. [PubMed: 16951960]
22. Krauzlis RJ. Population coding of movement dynamics by cerebellar Purkinje cells. Neuroreport. 2000; 11:1045–1050. [PubMed: 10790880]
23. Andersen RA, Essick GK, Siegel RM. Encoding of spatial location by posterior parietal neurons. Science. 1985; 230:456–458. [PubMed: 4048942]
24. Paninski L, Shoham S, Fellows MR, Hatsopoulos NG, Donoghue JP. Superlinear Population Encoding of Dynamic Hand Trajectory in Primary Motor Cortex. J. Neurosci. 2004; 24:8551–8561. [PubMed: 15456829]
25. Herzfeld DJ, Vaswani PA, Marko MK, Shadmehr R. A memory of errors in sensorimotor learning. Science. 2014; 345:1349–1353. [PubMed: 25123484]
26. Fuchs AF, Robinson DA. A method for measuring horizontal and vertical eye movement chronically in the monkey. J. Appl. Physiol. 1966; 21:1068–1070. [PubMed: 4958032]
27. McLaughlin SC. Parametric adjustment in saccadic eye movements. Percept. Psychophys. 1967; 2:359–362.
28. Lisberger SG, Pavelko TA. Vestibular signals carried by pathways subserving plasticity of the vestibulo-ocular reflex in monkeys. J. Neurosci. 1986; 6:346–354. [PubMed: 3485189]

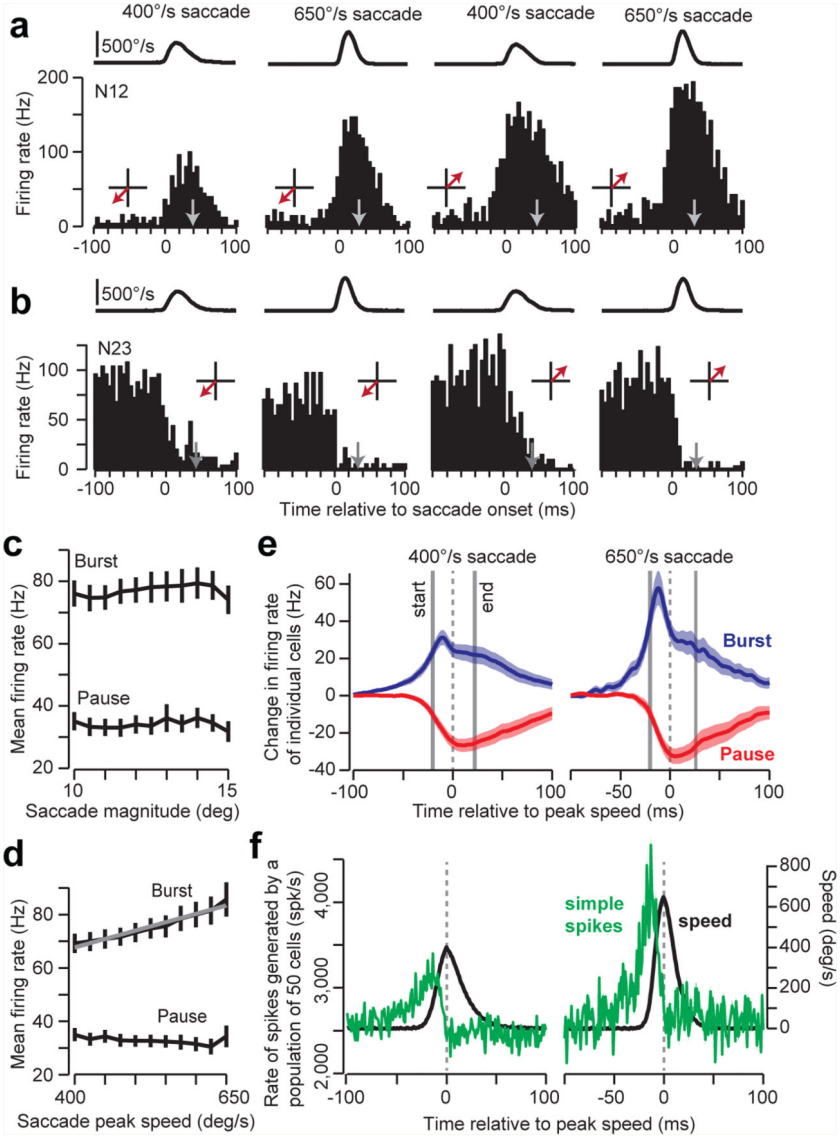

Figure 1.

Population of burst and pause P-cells together predict eye speed in real-time. Perisaccade histograms for a bursting (**a**) and pausing (**b**) P-cell during saccades of various speeds and directions (red arrow). The trace on the top row is saccade speed. The gray arrow indicates saccade end. **c and d.** Mean firing rates over the duration of saccade computed across all directions. Changes in speed produced an increase in the firing rate of the burst cells but not the pause cells. **e.** Change in firing rates (with respect to baseline) of the bursting and pausing P-cells for two saccade speeds. Gray bars are onset and termination of the saccade (width is SEM). **f.** The total rate of simple-spikes produced by a random selection of 50 P-cells.

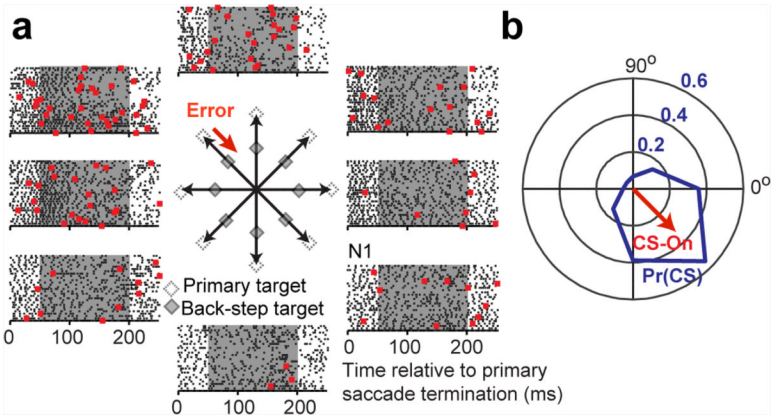

Figure 2.

Determination of complex-spike (CS) properties of P-cells. **a.** Response of a P-cell during the 250ms period after completion of a saccade (simple-spikes are gray, complex-spikes are red). CS-on was determined via a back-step paradigm in which the target was jumped (unfilled target to filled target) during saccade execution. Black arrow indicates saccade vector, red arrow indicates error vector. We computed the probability of CS in the 50-200ms period following saccade termination. **b.** The probability of a CS as a function of the direction of the error vector. For this neuron, the highest probability (CS-on) occurred when the error vector was in direction −45°. Direction of CS-off for this cell was 135°.

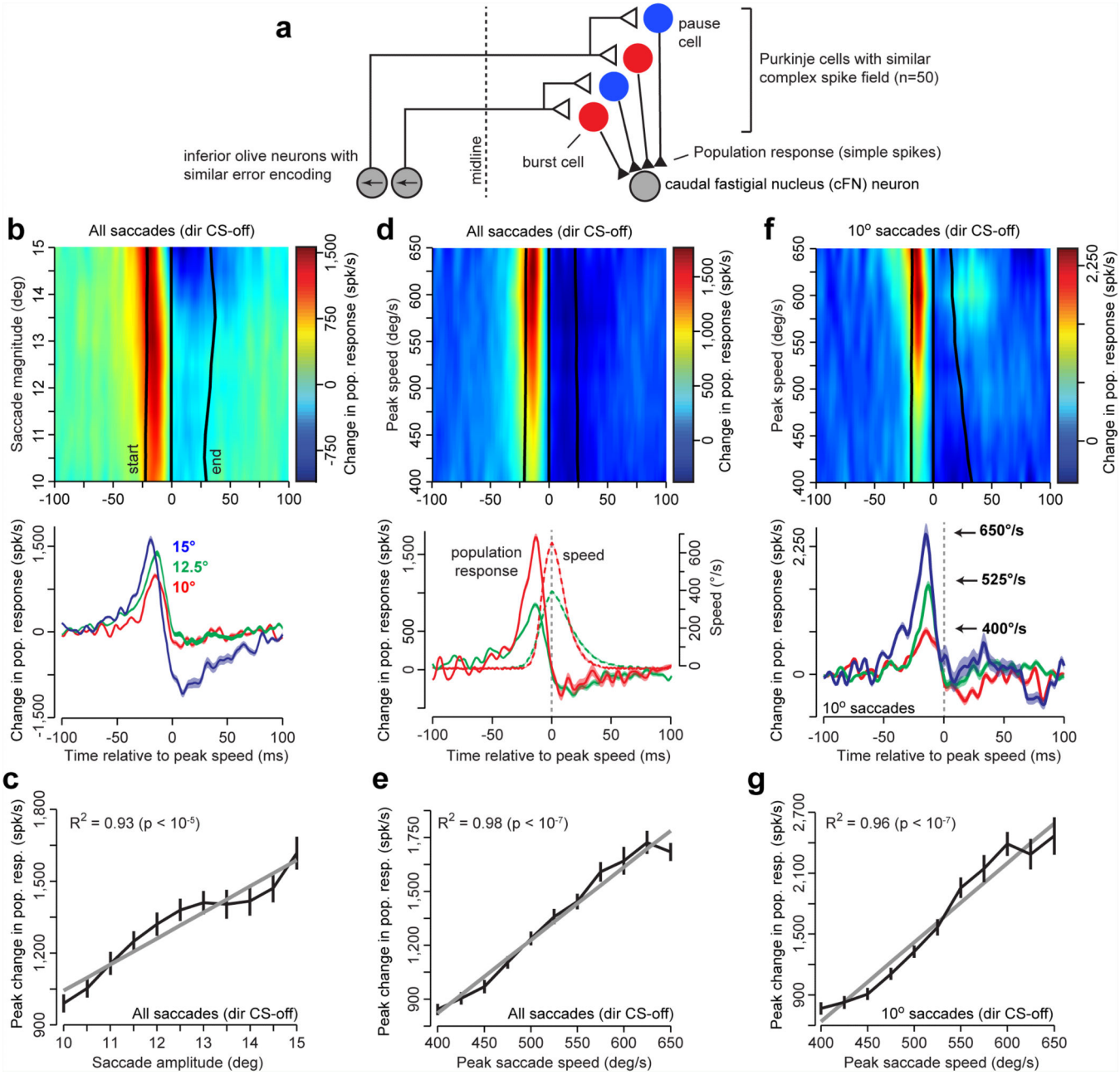

Figure 3.

Cluster of P-cells, organized by their complex-spikes, produced a population response that predicted in real-time the motion of the eye. **a.** Hypothesized organization of the oculomotor vermis. To compute a population response, we measured the simple-spikes of each P-cell as a function of saccade direction with respect to the CS-on direction of that cell. For the P-cells shown here, the CS-on is an error vector to the left (arrow). **b.** Change in population response (with respect to baseline) as a function of saccade amplitude in 0.5° bins, for saccades in the CS-off direction. Data in the amplitude axis were smoothed by a first-order Savitzky-Golay filter with a width of 3 bins[6]. Bottom plot shows the population response for three representative amplitudes. **c.** Peak population response increased linearly with saccade

amplitude. P-values indicates significant linear correlation. **d.** Population response as a function of saccade peak-speed. Bottom plot shows representative responses with their corresponding speed traces. **e.** Peak population response increased linearly with saccade peak-speed. **f.** Population response for 10° saccades (±1°), as a function of saccade peak-speed. Bottom plot shows the population response for slow, medium, and fast saccades of 10° amplitude. **g.** Peak population response increased linearly as a function of peak-speed even for a fixed magnitude saccade. Error bars are SEM.

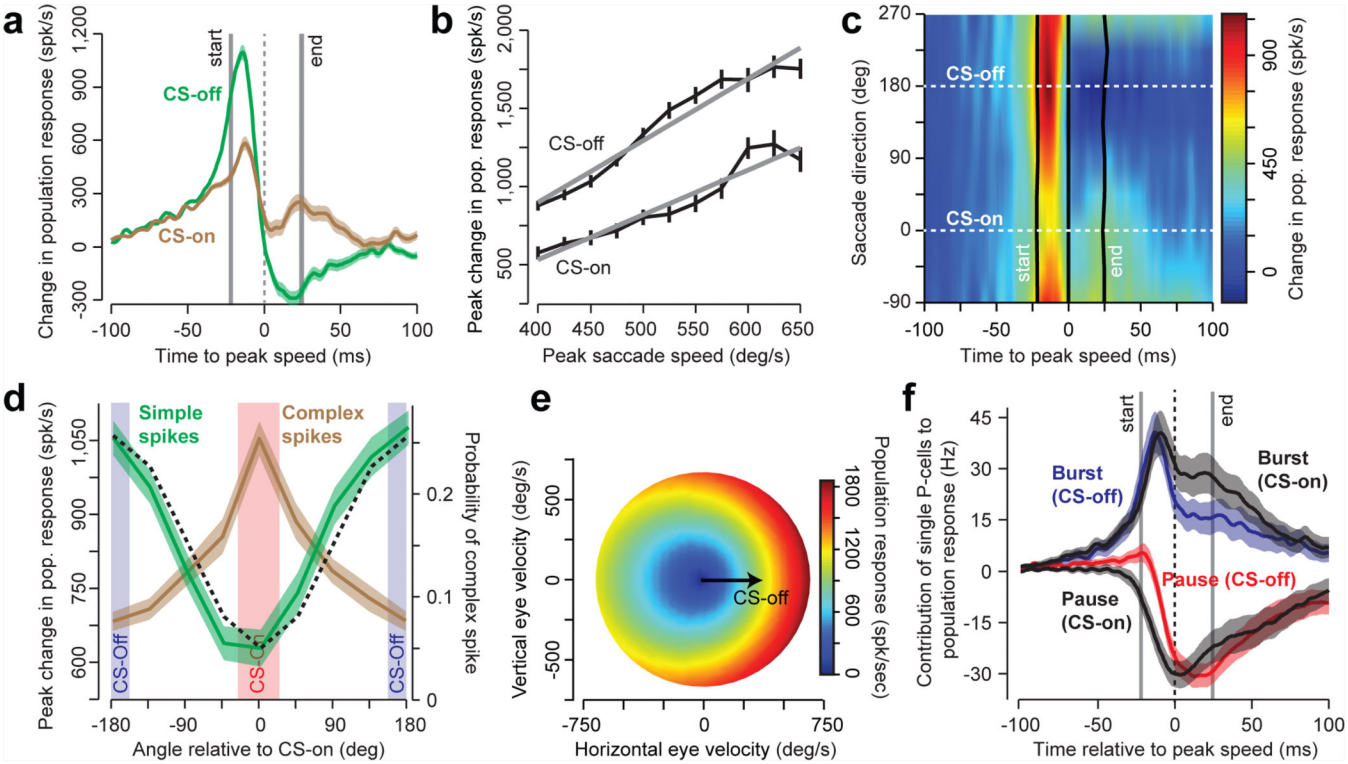

Figure 4.

Population response of P-cells predicted saccade speed and direction in real-time as a gain-field. **a.** Population response for saccades in direction CS-on and CS-off. The population response is larger when the saccade is in the CS-off direction. **b.** Peak population response grew linearly with saccade speed, but had a higher gain for saccades in CS-off direction. **c.** Real-time population response as a function of saccade direction relative to CS-on. Data smoothed as in Fig. 3b. **d.** Peak population response (labeled as simple-spikes) as a function of saccade direction with respect to CS-on. Brown curve shows probability of observing a complex-spike as a function of the angle relative to each neuron's CS-on. Black curve indicates cosine fit of probability of CS. **e.** Gain-field encoding by a cluster of P-cells whose CS-off direction is to the right (Eq. 1). **f.** Contribution of single P-cells to the population response. A change in direction coincides with a shift in timing of the pause cells. Error bars are SEM.